

## Abstract

We present recent efforts to use 3D Smoothed Particle Hydrodynamics (SPH) simulations to model the binary wind collision in Eta Carinae, with emphasis on reproducing BVRI photometric variations observed from La Plata Observatory. Photometric dips occurring concurrently with X-ray minima seen with RXTE provide further evidence for binarity in the system. We investigate the role of the unseen secondary star, focusing on two effects: 1) an occultation of the secondary by the slower, extended optically thick primary wind; and 2) a "Bore Hole" effect, wherein the fast wind from the secondary carves a cavity in the dense primary wind, allowing increased escape of radiation from the hotter/deeper layers of the primary's extended photosphere. Such models may provide clues on how/where light is escaping the system, the directional illumination of distant material (e.g., the big and little Homunculus, the "purple haze", Weigelt blobs, etc.), and the parameters/orientation of the binary orbit.

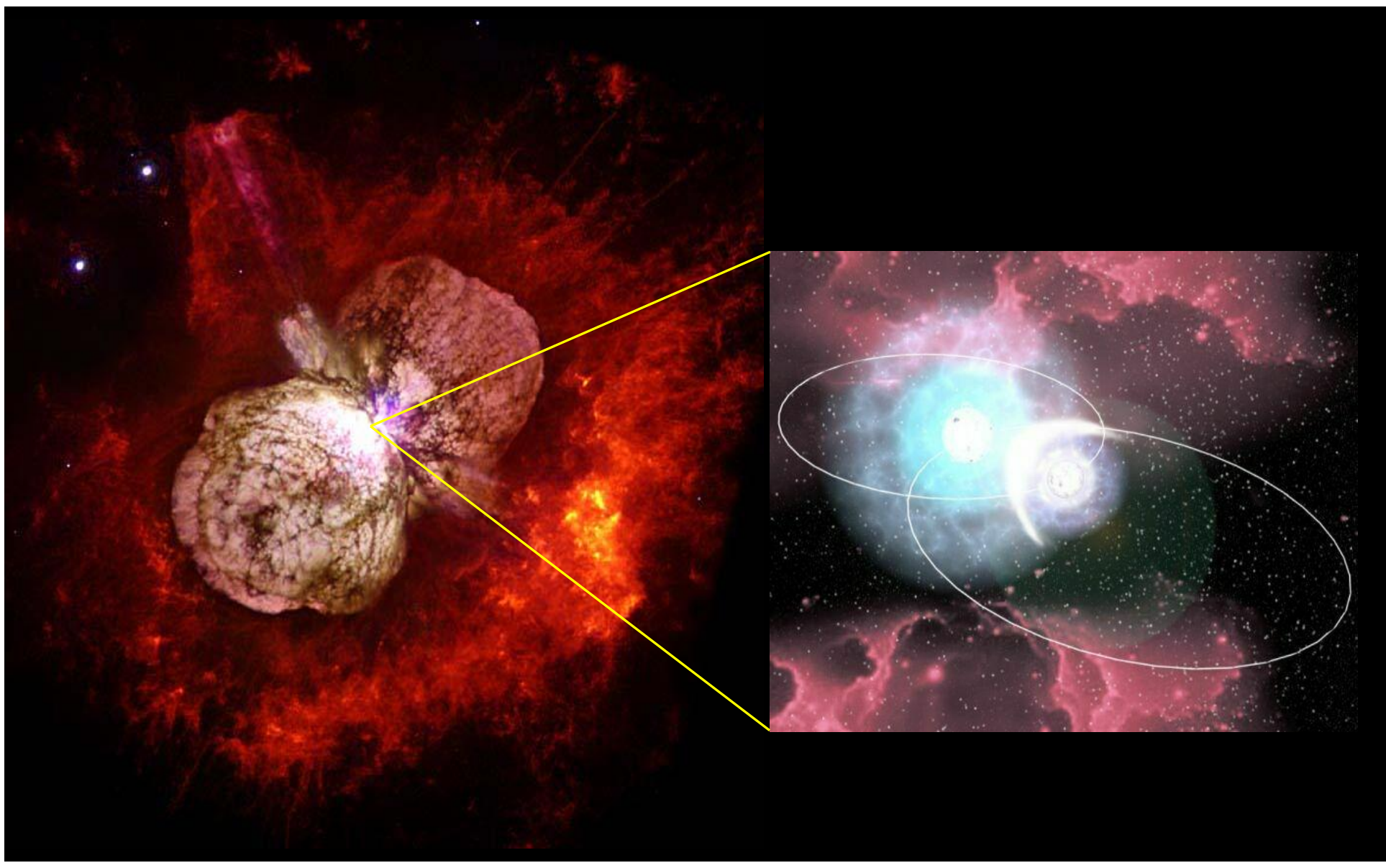


Figure 1: HST image of  $\eta$  Carinae (Nathan Smith/NASA) with artist's conception (Augusto Daminieli, www.etacarinae.iag.usp.br) of the interacting binary.

## The Observations

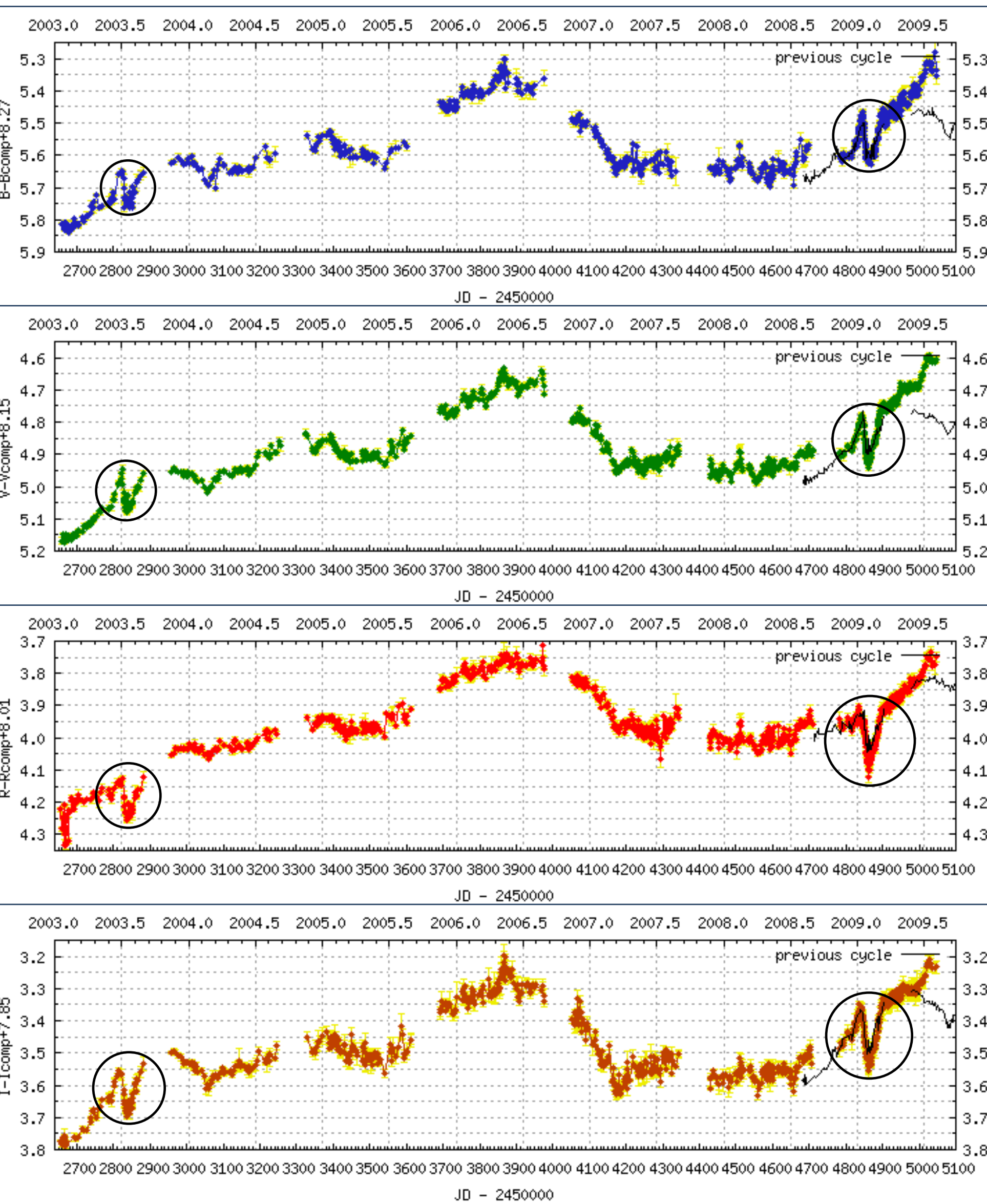


Figure 2: BVRI Differential Photometry of Eta Car observed from La Plata Observatory. Data is courtesy of Eduardo Fernández Lajús and is available at <http://etacar.fcaglp.unlp.edu.ar/>. We attempt to model the two eclipse-like events that occurred in 2003.5 and just after 2009.0 (circled above), which are likely due to the binarity of the system. Other changes in brightness appear to be secular, possibly due to changes in dust extinction from the Homunculus nebula and *not* the binary orbit. Note that we **do not** attempt to model these secular changes, only the eclipse-like events.

## Synthetic Light Curves

We generate synthetic light curves for various values of  $\kappa$  from 0.34–80  $\text{cm}^2 \text{g}^{-1}$  for both SPH models 1 & 2, for various lines-of-sight to the observer by: (1) creating a series of frames of surface brightness for each time step in the simulation, (2) summing over all pixel values in each frame to obtain a value of the apparent brightness, (3) converting each apparent brightness to a magnitude via Equation 3, and (4) plotting these magnitudes as a function of phase. Figure 9 compares light curves from both SPH models for similar values of the parameter  $\kappa M$  which best reproduce the observed eclipse-like events. **These model light curves reproduce the observed steep rise and drop before minimum, and give roughly the same peak-to-peak change in magnitude and "eclipse" duration.** Finally, Figure 10 is a light curve from a model of a simple occultation of the secondary by the extended, optically thick primary wind with no bore hole effect.

$$\Delta m = -2.5 \log_{10} \left[ \frac{L(t)}{L(t = \text{apastron})} \right]$$

Eq 3: Magnitude difference at time  $t$ , defined relative to the value at apastron, used in the synthetic light curves.

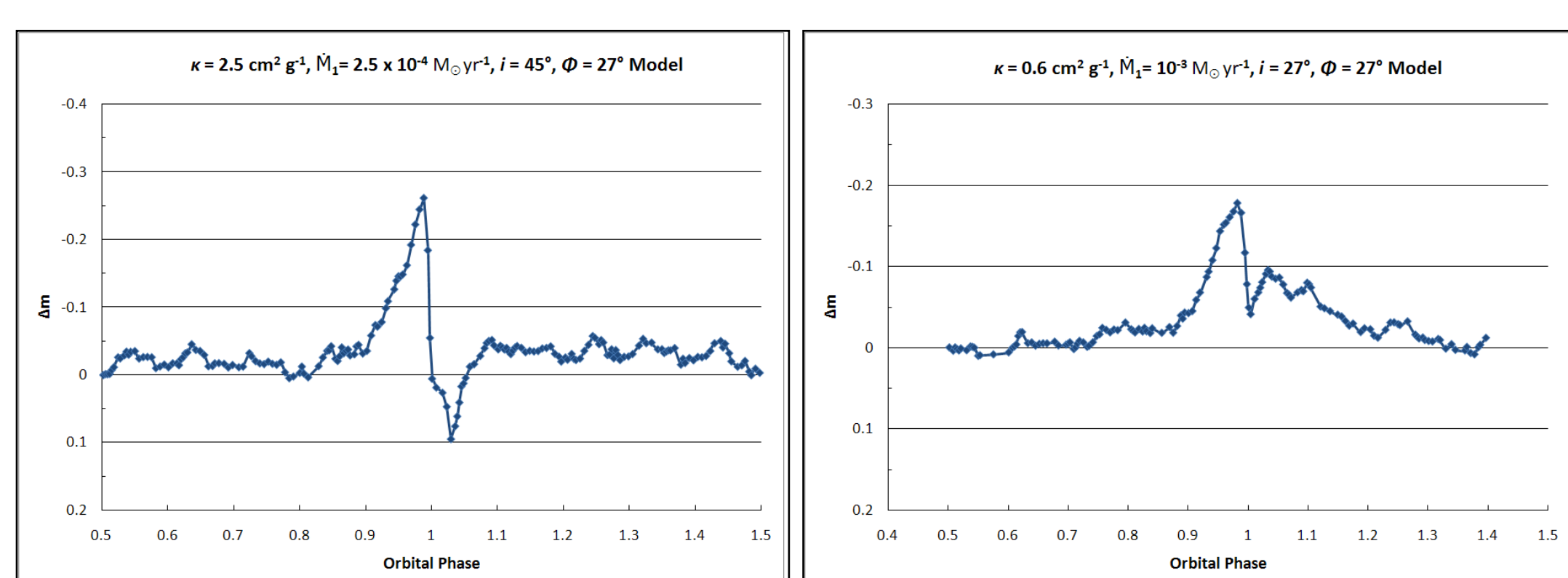


Figure 9: Synthetic light curves from both SPH models 1 & 2 for a constant value of the parameter  $\kappa M$ . The angle  $\phi$  is measured prograde relative to the orbital semi-major axis, while  $i$  is the inclination.

## Binarity and the Bore Hole Effect

Recently, Okazaki et al. (2008) modeled the RXTE X-ray light curve of Eta Car using a 3D SPH simulation of the binary wind-wind collision. A key point of their work is that the fast wind of the secondary star carves a cavity in the dense wind of the primary, allowing X-rays that would otherwise be absorbed to escape into our line-of-sight. If the primary wind is sufficiently optically thick in the optical or IR waveband, then the low-density secondary wind may likewise carve or "bore" a cavity or "hole" in the associated wind photosphere, allowing increased escape of radiation from the hotter/deeper layers.

A bore hole effect occurs if  $R_{\text{phot}} > R_{\text{min}}$ . For the parameters in Table 1, this is the case, even for low values of  $\kappa$  of order unity. Increasing  $\kappa$  (or equivalently  $M$ ) results in a larger primary star and a bore hole at phases other than periastron.

Table 1: 3D SPH Model Stellar/Wind Parameters	Primary Star	Secondary Star
Mass ( $M_{\odot}$ )	90	30
Radius ( $R_{\odot}$ )	90	30
Mass Loss Rate ( $M_{\odot}/\text{yr}$ )	$2.5 \times 10^{-4}$ (for model 1)	$1.0 \times 10^{-5}$
	$1.0 \times 10^{-3}$ (for model 2)	
Wind Speed (km/s)	500	3000
Temperature (K)	35,000	35,000
Particle Mass ( $M_{\odot}$ )	$6 \times 10^{-14}$	$1.2 \times 10^{-14}$
Eccentricity $e$	0.9	
Orbital Period	2024 days	
Semi-major axis length $a$	15.4 AU	

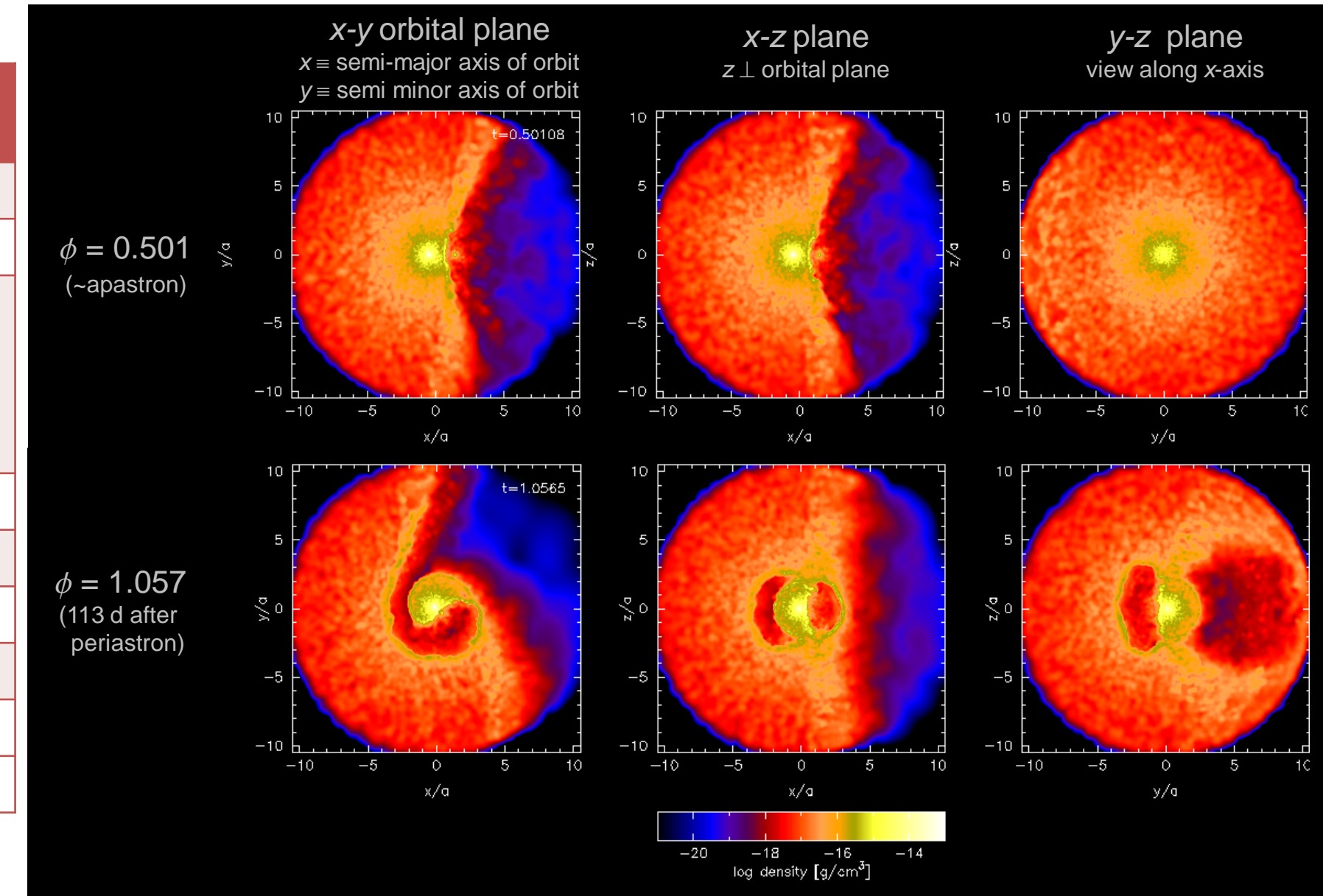


Figure 3: Snapshots for two phases from the 3D SPH simulation of the wind-wind collision in  $\eta$  Car using the parameters in Table 1 (model 1,  $\dot{M}_1 = 2.5 \times 10^{-4} M_{\odot}/\text{yr}$ ). At  $t = 0, 0.5$ , the system is at apastron.

## The Theory

Such a "bore hole" should depend on (1) how close the cavity carved by the secondary gets to the primary and (2) the apparent size of the primary photosphere. If at some point (2) > (1), there is a bore hole.

$$R_{\text{min}} \approx \frac{a(1-e)}{1+1/\sqrt{\eta}} \approx 1 \text{ AU}$$

Eq 1: Min distance from primary to head of shock cone at periastron for a wind momentum ratio of  $\eta \approx 4.2$ .  $a$  is the semi-major axis length and  $e$  the orbital eccentricity.

$$R_{\text{phot}} = \frac{\kappa \dot{M}_1}{4\pi v_1} \approx \frac{\kappa a}{10}$$

Eq 2: Apparent size of the primary, using the photospheric radius at which the optical depth  $\tau = 1$ .  $\kappa$  is the opacity in  $\text{cm}^2 \text{g}^{-1}$  and is assumed constant.

## The 3D SPH Models

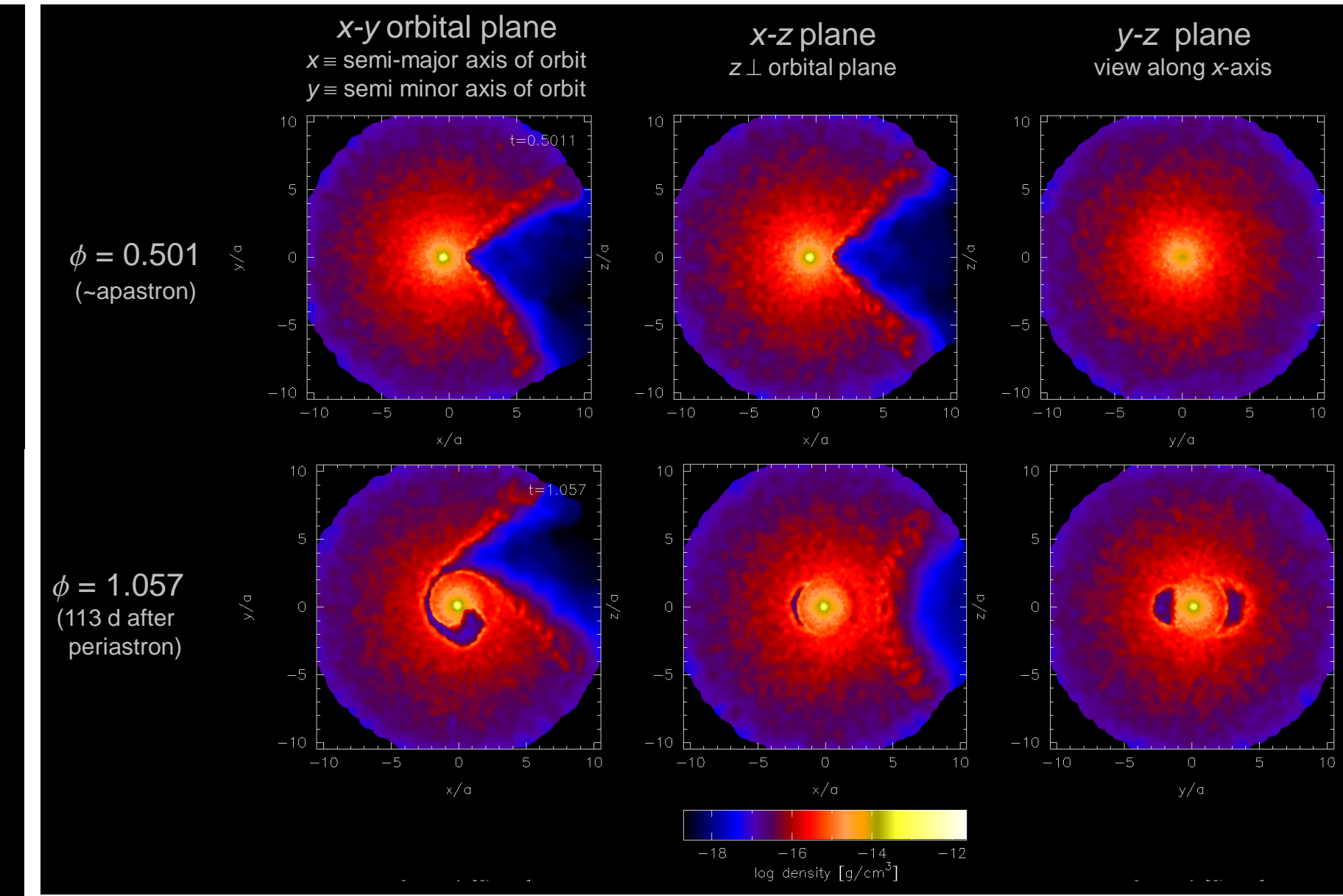


Figure 4: Snapshots for two phases from the 3D SPH simulation of  $\eta$  Car for model 2 ( $\dot{M}_1 = 10^{-3} M_{\odot}/\text{yr}$ ). Again, at  $t = 0, 0.5$ , the system is at apastron. Note the different, smaller shock opening angle versus model 1.

We use two 3D SPH simulations, each similar to that of Okazaki et al. (2008) (with the exception that the new models are adiabatic), combined with a modified version of the visualization program SPLASH (Price 2007), to generate renderings of surface brightness of the primary and secondary star for various values of the opacity  $\kappa$  (from 0.34–80  $\text{cm}^2 \text{g}^{-1}$ ) as a function of orbital phase for different binary system orientations relative to the observer's line-of-sight. In our SPLASH renderings, our first model ( $\dot{M}_1 = 2.5 \times 10^{-4} M_{\odot}/\text{yr}$ , Figures 5-7) assumes the observer's line-of-sight is the same as the best-fit from Okazaki et al. (2008), i.e., inclined  $45^\circ$  and rotated  $27^\circ$  prograde relative to the orbital semi-major axis. Model 2 ( $\dot{M}_1 = 10^{-3} M_{\odot}/\text{yr}$ ) assumes an observer's line-of-sight inclined  $27^\circ$  and rotated  $27^\circ$  prograde relative to the orbital semi-major axis. Our models reveal three possible bore hole scenarios, as illustrated in Figures 5-7. In each of these figures, the  $x$  and  $y$  axes are the major and minor axes of the orbit, respectively, and  $z$  is the orbital axis  $\perp$  to the orbital plane. Lengths in AU are indicated, as is the direction of North on the sky and the orbital phase ( $t=0.5$  &  $1.5$  for apastron;  $t=0, 1, 2$  for periastron). Color scale indicates surface brightness.

Figure 5: The "No Cavity" Scenario: Occurs for low values of  $\kappa$  (0.34  $\text{cm}^2/\text{g}$ , used here). The primary's photospheric radius is so small the head of the shock cone never penetrates and there is never a bore hole effect.

Figure 6: The "Moderate Cavity" Scenario: Found for intermediate values of  $\kappa$  (2.5–10  $\text{cm}^2/\text{g}$ ). At/near apastron, shock cone is too far from the primary and there is no bore hole (1<sup>st</sup> panel). As secondary moves closer during its orbit, shock cone gradually penetrates, creating a bore hole effect (2<sup>nd</sup> panel). During periastron, secondary wraps around the primary and bore hole briefly vanishes. After periastron, bore hole reappears on opposite side of the primary (3<sup>rd</sup> panel) and then fades as secondary moves back towards apastron (4<sup>th</sup> panel).

Figure 7: The "Large Cavity" Scenario: Occurs for high values of  $\kappa$  ( $\geq 20 \text{ cm}^2/\text{g}$ ). The primary's photosphere is so large the shock cone head penetrates at all orbital phases, creating a significant bore hole effect for the entire orbit (except when it briefly vanishes during periastron).

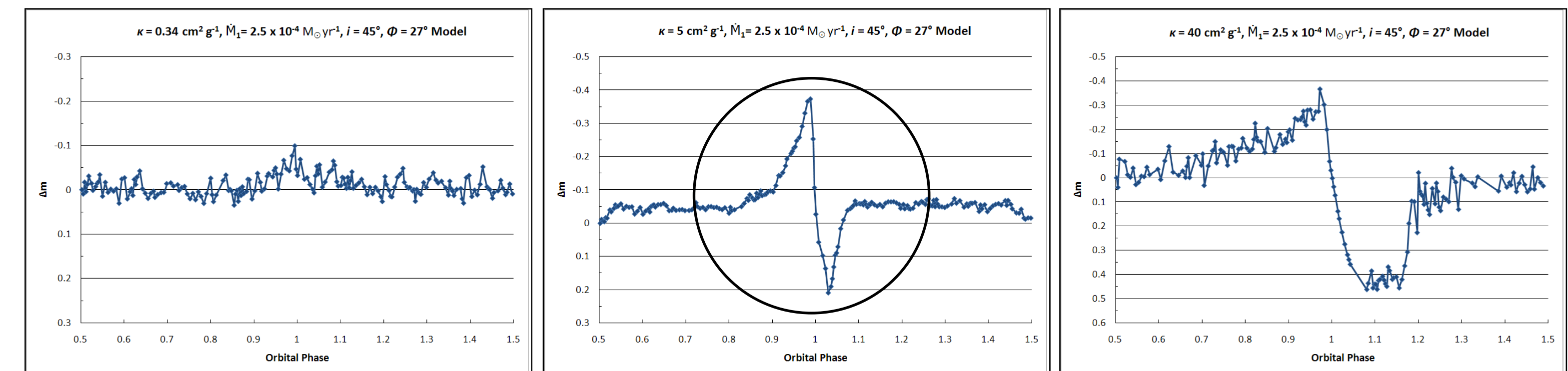
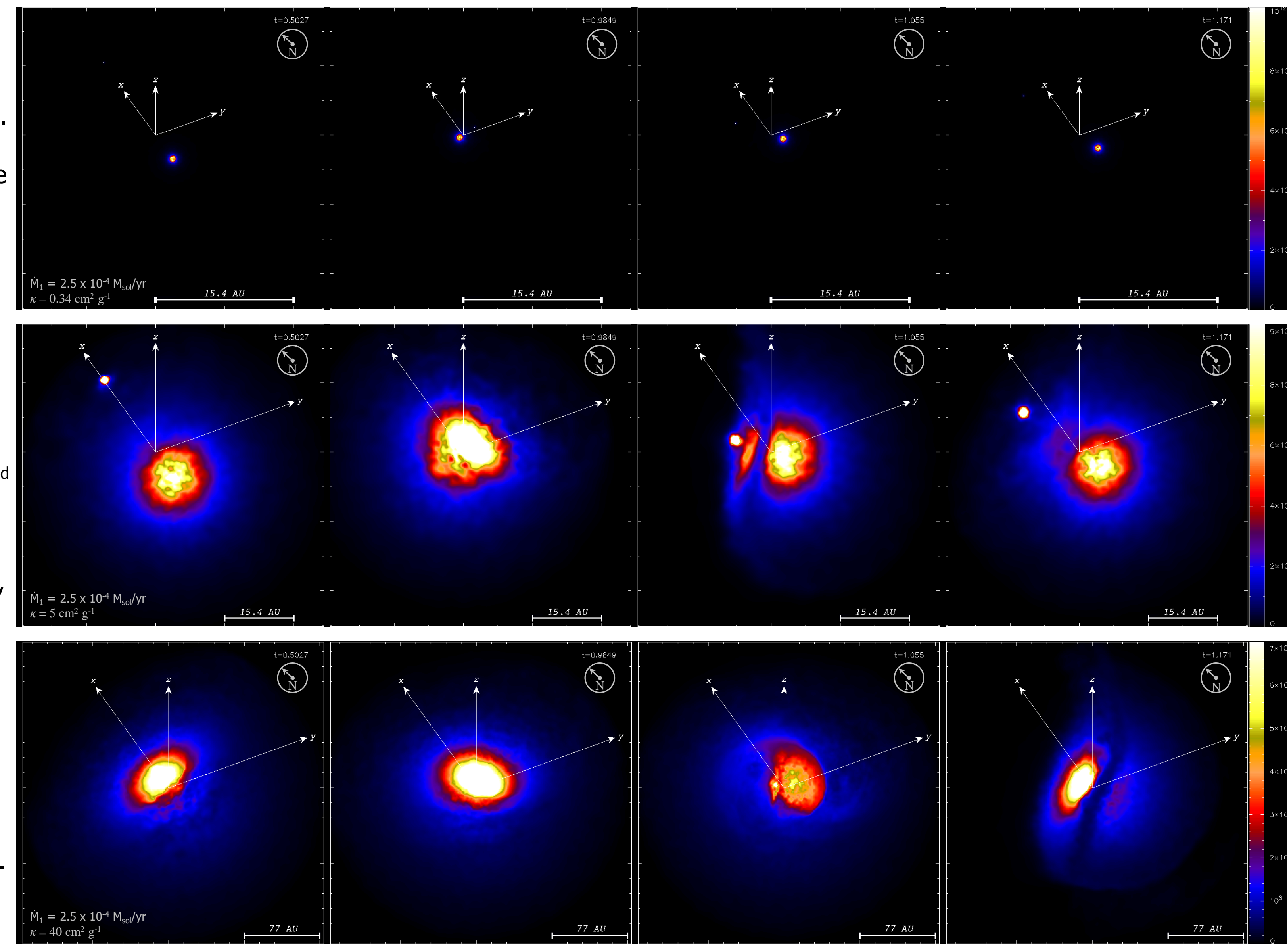


Figure 8: Synthetic light curves for the models of Figures 5-7 above.

## Conclusions and To Do List

- ❖ Of the models done so far, the "moderate cavity" bore hole scenario matches the data best, reproducing the observed steep rise and drop before minimum, and giving roughly the same peak-to-peak change in magnitude and "eclipse" duration.
- ❖ Model light curves support an observer's line-of-sight  $\sim 30^\circ$  prograde of the orbital semi-major axis & inclined  $30-45^\circ$ , similar to values found by Okazaki et al. (2008) & Parkin et al. (2009).
- ❖ A pure eclipse scenario of the secondary by the dense wind of the primary so far does not seem to match the observations, in particular, the steep rise seen just before minimum.
- ❖ Need a 3D aspherical wind SPH model. The above models assume spherically symmetric winds.
- ❖ Instead of a constant, parameterized opacity  $\kappa$ , need to use a physics-based opacity that depends on density, temperature and wavelength.

## References:

Fernández Lajús, E. 2009, <http://etacar.fcaglp.unlp.edu.ar/> and private communication.  
Okazaki, A. T., Owocki, S. P., Russell, C. M. P., & Corcoran, M. F. 2008, MNRAS, 388, L39  
Parkin, E. R., Pittard, J. M., Corcoran, M. F., Hamaguchi, K., Stevens, I. R. 2009, MNRAS, 394, 1758  
Price, D. J. 2007, Publications of the Astronomical Society of Australia, 24, 159